

p22^{phox} Is a Critical Component of the Superoxide-generating NADH/NADPH Oxidase System and Regulates Angiotensin II-induced Hypertrophy in Vascular Smooth Muscle Cells*

(Received for publication, June 11, 1996, and in revised form, July 17, 1996)

Masuko Ushio-Fukai, A. Maziar Zafari, Toshiki Fukui, Nobukazu Ishizaka, and Kathy K. Griendling‡

From the Department of Medicine, Division of Cardiology, Emory University, Atlanta, Georgia 30322

Superoxide anion formation is vital to the microbicidal activity of phagocytes. Recently, however, there is accumulating evidence that it is also involved in cell growth in vascular smooth muscle cells (VSMCs). We have shown that the hypertrophic agent angiotensin II stimulates superoxide production by activating the membrane-bound NADH/NADPH oxidase and that inhibition of this oxidase attenuates vascular hypertrophy. However, the molecular identity of this oxidase in VSMCs is unknown. We have recently cloned the cytochrome *b*₅₅₈ α -subunit, p22^{phox} (one of the key electron transfer elements of the NADPH oxidase in phagocytes), from a rat VSMC cDNA library, but its role in VSMC oxidase activity remains unclarified. Here we report that the complete inhibition of p22^{phox} mRNA expression by stable transfection of antisense p22^{phox} cDNA into VSMCs results in a decrease in cytochrome *b* content, which is accompanied by a significant inhibition of angiotensin II-stimulated NADH/NADPH-dependent superoxide production, subsequent hydrogen peroxide production, and [³H]leucine incorporation. We provide the first evidence that p22^{phox} is a critical component of superoxide-generating vascular NADH/NADPH oxidase and suggest a central role for this oxidase system in vascular hypertrophy.

Superoxide anion (O₂⁻) formation is known to be vital to the microbicidal activity of phagocytes such as neutrophils, macrophages, and monocytes (1). Recently, however, it has become apparent that production of reactive oxygen species also occurs in non-phagocytic cells such as fibroblasts (2), glomerular mesangial cells (3), endothelial cells (4), and smooth muscle cells (5) and that it plays a role in cell growth in some systems. In tumor cells, antitumor agents inhibit the plasma membrane redox system (6), while in cultured VSMCs,¹ hydrogen peroxide (H₂O₂) and xanthine/xanthine oxidase, which produces H₂O₂ and O₂⁻, stimulate cell proliferation and induce the expression of growth-related genes, including *c-fos*, *c-myc*, and *c-jun* (7–9). Furthermore, treatment of VSMCs with antioxidants induces

apoptosis, implying that reactive oxygen species may be necessary for normal proliferation (10).

We have previously demonstrated that in cultured VSMCs, the hypertrophic agent angiotensin II (Ang II) causes a delayed, sustained O₂⁻ production by activating a membrane-associated NADH/NADPH oxidase (5). This enzyme appears to be the major source of O₂⁻ in this cell type and appears to play a role in Ang II-induced hypertrophy (5). However, the molecular identity of this oxidase in VSMCs is unknown. Although an NADPH oxidase system has been well characterized in phagocytic cells, where it consists of cytosolic components, p47^{phox} and p67^{phox} (11, 12), a low molecular weight G-protein, Rac 1 or Rac 2 (13, 14), and a membrane-associated cytochrome *b*₅₅₈ (15), the structural and functional characteristics of this oxidase appear to be different from those seen in non-phagocytic cells (3, 16–21). In phagocytes, cytochrome *b*₅₅₈ functions as the final electron transporter from NADPH to molecular oxygen, and this protein consists of a 22-kDa α -subunit (p22^{phox}) and a glycosylated 91-kDa β -subunit (gp91^{phox}) (15). In non-phagocytic cells, p22^{phox} has been detected using reverse transcriptase-polymerase chain reaction, but there is no evidence for the presence of gp91^{phox}, and it has been suggested that the cytochrome *b*₅₅₈ is a variant of the phagocytic form (22). Furthermore, although p22^{phox} has been shown to be expressed, a functional role for this protein in O₂⁻ generation has not been demonstrated.

In cultured VSMCs, the NADH/NADPH oxidase preferentially utilizes NADH as opposed to NADPH as a substrate (5), which is in marked contrast to the phagocytic enzyme. This observation is similar to those made in pulmonary and coronary arteries, where a cytochrome *b*₅₅₈-based microsomal NADH oxidase accounts for the vast majority of O₂⁻ production (23, 24). These data raise the possibility that the VSMC NADH oxidase may be the same enzyme, or at least utilize the same cytochrome *b*₅₅₈ electron transport system, as the VSMC NADPH oxidase.

We have recently cloned p22^{phox} from a rat VSMC cDNA library and found that it bears a high homology to the human neutrophil nucleotide sequence (25), but its role in VSMC oxidase activity is unclear. In this report, to test the hypothesis that p22^{phox} is an essential component of the vascular NADH/NADPH oxidase and that this oxidase system plays a role in Ang II-induced hypertrophy in VSMCs, we stably transfected antisense p22^{phox} cDNA into rat aortic smooth muscle cells. Our data strongly suggest that VSMCs utilize a p22^{phox}-containing, cytochrome *b*₅₅₈-like protein to transfer electrons from both NADH and NADPH to oxygen and provide evidence for a central role of this oxidase system in signal transduction related to vascular cell growth.

* This work was supported by National Institutes of Health Grant HL38206. The costs of publication of this article were defrayed in part by the payment of page charges. This article must therefore be hereby marked "advertisement" in accordance with 18 U.S.C. Section 1734 solely to indicate this fact.

‡ To whom correspondence should be addressed: Division of Cardiology, Emory University School of Medicine, 319 WMB, 1639 Pierce Dr., Atlanta, GA 30322. Tel.: 404-727-8168; Fax: 404-727-3330; E-mail: kgriend@emory.edu.

¹ The abbreviations used are: VSMC, vascular smooth muscle cell; Ang II, angiotensin II; O₂⁻, superoxide anion; H₂O₂, hydrogen peroxide; DMEM, Dulbecco's modified Eagle's medium; DPI, diphenylene iodonium; DCF-DA, 2',7'-dichlorofluorescein diacetate.

EXPERIMENTAL PROCEDURES

Materials—pSPORT and pcDNA3 vectors were from Invitrogen (San Diego, CA). Bovine serum albumin and phenylmethanesulfonyl fluoride were from Boehringer Mannheim. Lipofectin, geneticin, soybean trypsin inhibitor, glutamine, penicillin, streptomycin, and trypsin-EDTA were purchased from Life Technologies, Inc. (Gaithersburg, MD). TRI reagent was from Molecular Research Center (Cincinnati, OH). Prime-It II kit was from Stratagene (Menasha, WI). Liquiscint was purchased from National Diagnostics (Atlanta, GA), and [³H]leucine (140 Ci/mmol) was from DuPont NEN. 2',7'-Dichlorofluorescein diacetate (DCF-DA) was from Molecular Probes (Eugene, OR). Common buffer salts were obtained from Fisher. All other chemicals and reagents, including Dulbecco's modified Eagle's medium (DMEM) with 25 mM Hepes and 4.5 g/liter glucose and calf serum, were from Sigma. Losartan was a kind gift from Dr. R. D. Smith (DuPont de Nemours Co.).

Cell Culture—VSMCs, isolated from male Sprague-Dawley rat thoracic aortas by enzymatic digestion, were grown in DMEM supplemented with 10% calf serum, as described previously (26).

Construction and Transfection of Antisense p22^{phox} Expression Plasmid—A full-length p22^{phox} cDNA, cloned in the pSPORT vector, was digested with *SalI* and *NotI*. The *SalI/NotI*-cut p22^{phox} cDNA fragment (465 base pairs) was gel purified and ligated into the *NotI/XhoI* site of pcDNA3 in an antisense orientation. This ligation reaction could be accomplished because *XhoI* produces compatible ends with *SalI*. Transcription of the antisense p22^{phox} cDNA was under control of the cytomegalovirus immediate-early gene enhancer/promoter. This vector also contains a neomycin resistance gene, allowing selection of transfected cells with geneticin. Plasmid DNA was purified from ampicillin-resistant clones, and insertion of p22^{phox} cDNA was confirmed by restriction mapping. Four μ g of purified pcDNA3 alone or pcDNA3/antisense-p22^{phox} plasmid was suspended in 100 μ l of H₂O and gently mixed with a Lipofectin solution (100 μ l), and the formed DNA-liposome complex was added directly to 40–50% confluent VSMCs plated in 60-mm dishes in serum-reduced DMEM. Transfected VSMCs were incubated for 18 h at 37 °C, and then the medium was changed to DMEM containing 20% fetal bovine serum. After 48 h, transfected VSMCs were split 1:3 into 100-mm dishes and incubated in DMEM containing 10% fetal bovine serum and 400 μ g/ml geneticin. Eight days after selection, geneticin-resistant clones were isolated and amplified. Transfected cells were maintained in selection medium until they were plated into 35- or 100-mm dishes for experiments.

RNA Isolation and Northern Blot Analysis—Total RNA was isolated using the single-step TRI reagent, and 10 μ g of RNA was separated by 1% denaturing formaldehyde-agarose gels. Northern blotting was performed as described previously (27). The probe, a full-length rat p22^{phox} cDNA (25), was labeled with [α -³²P]dCTP using a random primer labeling kit (Prime-It II). After autoradiography, the relative density of each band was determined using laser densitometry. Staining of the 28 S band by ethidium bromide, after transfer to the membrane, was used for normalization.

Measurement of Cytochrome b-type Protein Expression—Membrane fractions were obtained from transfected VSMCs as follows. Cells were scraped in ice-cold phosphate-buffered saline and centrifuged at 750 \times g for 10 min at 4 °C. The pellet was resuspended and then underwent Dounce homogenization in ice-cold lysis buffer (20 mM monobasic potassium phosphate, pH 7.0, 1 mM EGTA, 10 μ g/ml aprotinin, 0.5 μ g/ml leupeptin, 0.7 μ g/ml pepstatin, 0.5 mM phenylmethanesulfonyl fluoride). The homogenate was centrifuged at 29,000 \times g for 20 min at 4 °C. The resulting membrane pellet was dissolved in ice-cold 100 mM sodium phosphate buffer (pH 7.2) containing protease inhibitors, underwent Dounce homogenization, and was incubated with agitation in 2% reduced Triton X-100 for 1 h at 4 °C. The insoluble fraction was pelleted by centrifugation at 29,000 \times g for 20 min at 4 °C, and the supernatant was transferred to an ultracentrifuge for centrifugation at 117,000 \times g for 70 min at 4 °C. The resulting supernatant containing solubilized cytochromes consisted of ~2.0 mg/ml protein. The reduced minus oxidized difference spectra of solubilized VSMC membranes were recorded on 1-ml samples (2.0 mg/ml) with a dual beam scanning spectrophotometer (Perkin-Elmer Lambda 2S) as described by Jones *et al.* (22). The base-line (oxidized) spectrum was recorded over 520–590 nm, a few grains of sodium dithionite were added to the sample cuvette, and a new spectrum was recorded when the cytochrome reached a completely reduced form. Subtraction was performed electronically.

NADPH/NADH Oxidase Assay—NADPH and NADH oxidase activity was measured using the O₂⁻-specific probe lucigenin, as described previously (5). Photon emission was measured every 15 s for 10–15 min

in a luminometer. The initial rate of enzyme activity was calculated by linear regression. A buffer blank (<5% of the cell signal) was subtracted from each reading prior to transformation of the data to nanomoles of O₂⁻, using a standard curve generated with xanthine/xanthine oxidase.

Measurements of Intracellular H₂O₂ Levels—Cells were plated at low density, grown for 48 h in culture medium containing 10% calf serum, and grown for an additional 24 h in culture medium containing 0.1% calf serum. Cells were stimulated with 100 nM Ang II for 4 h and incubated with the H₂O₂-sensitive fluorophore DCF-DA (28) for 30 min at room temperature and imaged by laser confocal scanning microscopy (MRC-1000, Bio-Rad). Relative DCF-DA fluorescence intensity was recorded. Although DCF-DA is oxidized by both H₂O₂ and other peroxides, the complete inhibition of fluorescence in Ang II-stimulated cells loaded with catalase indicates that the fluorescence signal evoked by Ang II is predominantly derived from H₂O₂ (data not shown).

[³H]Leucine Incorporation—VSMCs were plated at low density, grown for 48 h in culture medium containing 10% calf serum, and grown for an additional 72 h in culture medium containing 0.1% calf serum. Cells were incubated with [³H]leucine (0.5 μ Ci/ml) in the presence or absence of 100 nM Ang II for 24 h and then harvested, as described previously (5).

RESULTS AND DISCUSSION

To determine the function of p22^{phox} in the vascular NADH/NADPH oxidase system, we made an antisense p22^{phox} cDNA construct and stably transfected it into rat aortic smooth muscle cells (Fig. 1A). Control cells were transfected with vector only. The efficacy of antisense p22^{phox} cDNA transfection was evaluated by Northern analysis (Fig. 1B). Endogenous p22^{phox} mRNA was clearly expressed in cells transfected with vector alone and was similar to levels in non-transfected VSMCs (data not shown). In contrast, the 28 clones isolated from antisense p22^{phox}-transfected cells showed different levels of inhibition of p22^{phox} mRNA levels. One clone showed complete inhibition (A2 in Fig. 1B), and this clone was amplified and used for further study. The presence of antisense mRNA, as assessed by hybridization with a probe directed against the geneticin-resistant portion of the vector, correlated well with the inhibition of endogenous p22^{phox} mRNA (data not shown).

Since p22^{phox} is one subunit of cytochrome b₅₅₈, we examined the effects of disruption of p22^{phox} mRNA on cytochrome b content in membranes of antisense p22^{phox}-transfected cells as a measure of functional enzyme expression. In membranes of vector-transfected cells, we successfully detected a cytochrome peak at ~558 nm (Fig. 2). This is the first demonstration showing the presence of cytochrome b₅₅₈-like protein in VSMCs. In antisense p22^{phox}-transfected cells, this peak was dramatically decreased, indicating that p22^{phox} is part of the VSMC cytochrome b₅₅₈ complex.

To determine the role of p22^{phox} in Ang II-stimulated NADH/NADPH oxidase activity, we measured NADPH- and NADH-dependent O₂⁻ production in antisense p22^{phox}-transfected cells (Fig. 3A). Although the extent of O₂⁻ production in response to Ang II was much higher when NADH was used as a substrate, both Ang II-stimulated NADPH- and NADH-dependent O₂⁻ production were significantly inhibited in a parallel manner in antisense p22^{phox}-transfected cells (52.6 \pm 13.3% (n = 15, p < 0.05) and 54.0 \pm 11.8% (n = 15, p < 0.05), respectively). This partial inhibition of the oxidase activity in p22^{phox}-deficient cells is consistent with our previous findings that Ang II-stimulated NADH/NADPH oxidase activity was partially inhibited by diphenylene iodonium (DPI) (5), a known inhibitor of the flavoprotein component of the neutrophil NADPH oxidase. The remaining p22^{phox}-independent oxidase activity is most likely due to another NADH/NADPH-dependent oxidase, perhaps a constitutive one, since base-line oxidase activity was similar in vector- and antisense p22^{phox}-transfected cells. In other antisense p22^{phox}-transfected clones in which endogenous p22^{phox} mRNA expression was incompletely inhibited (A1 in Fig. 1B, for example), Ang II-stimulated oxidase activity was also in-

FIG. 1. Effect of stable transfection of an antisense p22^{phox} cDNA construct on endogenous p22^{phox} mRNA expression in VSMCs. A, schematic diagram of the construction of antisense p22^{phox} expression plasmid. The cloning vector, pSPORT, in which a full-length p22^{phox} cDNA was inserted, was digested with *Sal*I and *Not*I, and this p22^{phox} cDNA restriction fragment (465 base pairs (bp)) was ligated in an antisense orientation into the expression vector, pcDNA3, which was digested with *Xho*I and *Not*I. *CMV*, cytomegalovirus immediate-early gene enhancer/promoter; *SV40 ori*, SV40 origin for episomal replication; *Amp^r*, ampicillin resistance gene; *Neo^r*, geneticin resistance gene. B, Northern blot analysis of endogenous p22^{phox} mRNA levels in rat VSMC stably transfected with antisense p22^{phox} cDNA. Ten μ g of total RNA was used in each lane. Northern blot analysis was performed using full-length rat p22^{phox} cDNA as a probe. The upper panel shows a representative autoradiogram of endogenous p22^{phox} mRNA levels in vector-transfected clones (C1 and C2) and selected antisense p22^{phox}-transfected clones (A1, A2, and A3). The size of the p22^{phox} mRNA band is 0.8 kilobase (kb). The lower panel shows the 28 S ribosomal RNA band (detected by ethidium bromide fluorescence of the membrane).

FIG. 1. Effect of stable transfection of an antisense p22^{phox} cDNA construct on endogenous p22^{phox} mRNA expression in VSMCs. A, schematic diagram of the construction of antisense p22^{phox} expression plasmid. The cloning vector, pSPORT, in which a full-length p22^{phox} cDNA was inserted, was digested with *Sal*I and *Not*I, and this p22^{phox} cDNA restriction fragment (465 base pairs (bp)) was ligated in an antisense orientation into the expression vector, pcDNA3, which was digested with *Xho*I and *Not*I. *CMV*, cytomegalovirus immediate-early gene enhancer/promoter; *SV40 ori*, SV40 origin for episomal replication; *Amp^r*, ampicillin resistance gene; *Neo^r*, geneticin resistance gene. B, Northern blot analysis of endogenous p22^{phox} mRNA levels in rat VSMC stably transfected with antisense p22^{phox} cDNA. Ten μ g of total RNA was used in each lane. Northern blot analysis was performed using full-length rat p22^{phox} cDNA as a probe. The upper panel shows a representative autoradiogram of endogenous p22^{phox} mRNA levels in vector-transfected clones (C1 and C2) and selected antisense p22^{phox}-transfected clones (A1, A2, and A3). The size of the p22^{phox} mRNA band is 0.8 kilobase (kb). The lower panel shows the 28 S ribosomal RNA band (detected by ethidium bromide fluorescence of the membrane).

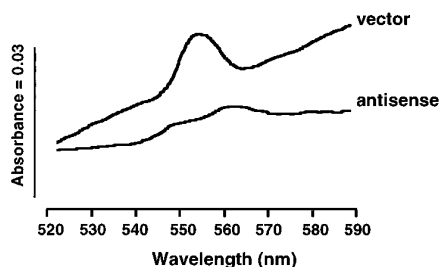
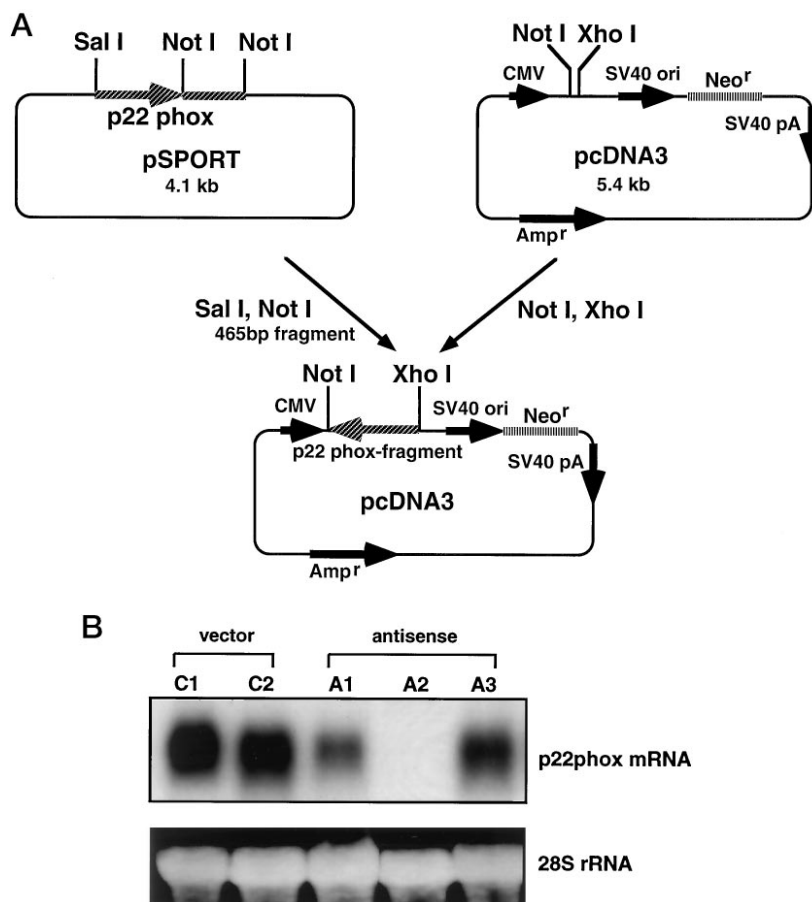


FIG. 2. Expression of cytochrome b-type protein in vector- and antisense p22^{phox}-transfected cells. Sodium dithionite-reduced minus oxidized difference spectra of membranes (0.2 mg of protein) obtained from vector- and antisense p22^{phox}-transfected cells are shown. Data are representative recordings obtained from two independent experiments.

hibited but to a lesser extent than that observed in the p22^{phox}-deficient clone (data not shown).

Since O₂⁻ is rapidly dismutated to hydrogen peroxide (H₂O₂), which also plays an important role in cell growth (7–9), we measured intracellular H₂O₂ levels ([H₂O₂]_i) in antisense p22^{phox}-transfected cells (Fig. 3B). [H₂O₂]_i, as measured by oxidation of the peroxide-sensitive fluorophore DCF-DA, was markedly increased by Ang II in vector-transfected cells. This increase in [H₂O₂]_i is most likely derived from O₂⁻ generated via activation of the NADH/NADPH oxidase by Ang II, as it is inhibited by 10 μ M DPI (data not shown). As expected, the Ang II-stimulated increase in [H₂O₂]_i in antisense p22^{phox}-transfected cells was dramatically decreased.

We also examined the effect of inhibition of the p22^{phox}-containing NADH/NADPH oxidase on Ang II-induced hypertrophy (Fig. 4). Ang II-stimulated [³H]leucine incorporation was significantly inhibited in antisense p22^{phox}-transfected

cells (52.0 \pm 8.3%, n = 4, p < 0.05) and was inhibited by losartan, an angiotensin type I receptor antagonist, to almost basal levels in vector- and antisense p22^{phox}-transfected cells, indicating that the response is mediated by AT₁ receptors.

To rule out the possibility that Ang II receptor expression or coupling might be decreased in antisense p22^{phox}-transfected cells, we measured Ang II-stimulated phospholipase D activity, an unrelated signaling event, and verified that Ang II-stimulated phospholipase D activity was not decreased in antisense p22^{phox}-transfected cells (411 \pm 29% of control, n = 3) as compared with vector-transfected cells (332 \pm 22% of control, n = 3). Furthermore, stimulation of NADH- and NADPH-dependent O₂⁻ production by arachidonic acid (which bypasses the receptor), was also significantly inhibited in antisense p22^{phox}-transfected cells (67.2 \pm 0.3% (n = 3, p < 0.05) and 48.9 \pm 6.4% (n = 4, p < 0.05), respectively). These results indicate that the physiological effects of antisense p22^{phox} transfection are in fact due to altered expression of the p22^{phox}-containing oxidase.

The p22^{phox} in phagocytes has been shown to play a pivotal role in the normal functioning of the NADPH oxidase (29–31). Our results suggest that p22^{phox} also plays an important role in NADPH-dependent O₂⁻ production in VSMCs. This is the first direct evidence that phagocytic oxidase components are *functional* in non-phagocytic cells. Furthermore, the activity of the NADH oxidase, which is a main source of superoxide production in cultured VSMCs (5) and pulmonary artery (23, 24), was also inhibited in p22^{phox}-deficient cells (Fig. 3A), suggesting that the VSMC p22^{phox} may be one of the components of both the NADH and NADPH oxidases or that one enzyme utilizes both substrates.

Functionally, the VSMC NADH/NADPH oxidase is similar to the NADPH oxidase identified in human fibroblasts (16) and mesangial cells (3). Both cells have a similar cytochrome *b*₅₅₈-

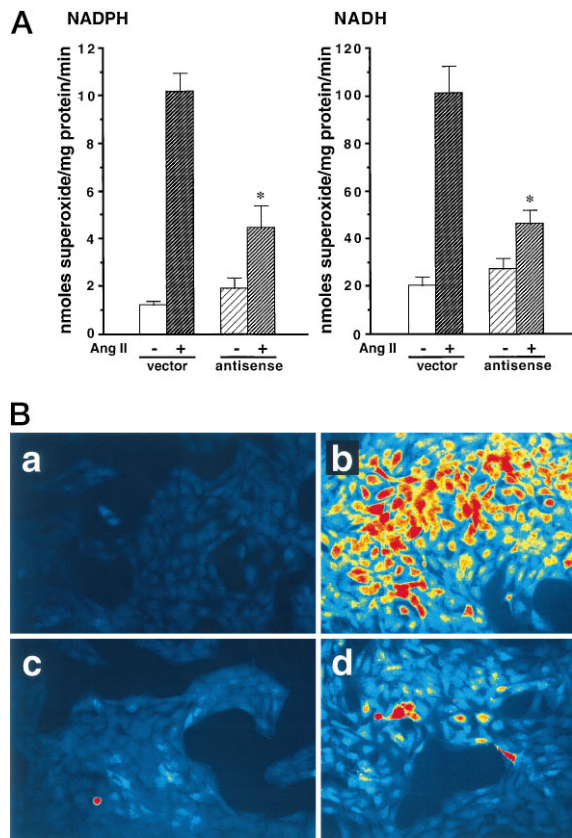


FIG. 3. NADH/NADPH oxidase activity and hydrogen peroxide (H₂O₂) production stimulated by Ang II in vector- and antisense p22^{phox}-transfected VSMCs. *A*, initial rate of NADPH- (left panel) and NADH- (right panel) dependent O₂⁻ production in vector- and antisense p22^{phox}-transfected cells stimulated with 100 nM Ang II for 4 h, as measured by lucigenin assay. - and + indicate treatment with vehicle or Ang II, respectively. The initial rate of enzyme activity was calculated over the first 30–120 s of exposure to NADPH or NADH and is expressed as nanomoles of superoxide/min/mg of protein. Statistical analysis was performed by Student's *t* test. Values are expressed as mean ± S.E. (*n* = 15). *, *p* < 0.05 for increase by Ang II in antisense- versus vector-transfected cells. *B*, increase in intracellular H₂O₂ levels in vector- and antisense p22^{phox}-transfected cells stimulated with 100 nM Ang II for 4 h, as measured by confocal microfluorometry. *a* and *b*, vector-transfected cells stimulated with vehicle or Ang II, respectively. *c* and *d*, antisense p22^{phox}-transfected cells stimulated with vehicle or Ang II, respectively.

like activity to that in VSMCs (Fig. 2), but the structure of cytochrome *b*₅₅₈ in these cells is different from that in phagocytes (3, 18). It is unlikely that p22^{phox} serves as a complete oxidase on its own, since it can only function as a one-electron acceptor and lacks substrate binding sites and flavin binding sites (20, 25). In VSMCs, we have been unable to detect the other subunit of cytochrome *b*₅₅₈, gp91^{phox}, using reverse transcriptase-polymerase chain reaction in VSMCs (data not shown). Therefore, the other subunit of the membrane NADH/NADPH oxidase in VSMCs may be structurally distinct from that in phagocytes, as suggested in other non-phagocytic cells (22). This notion is supported by the slight leftward shift of the peak of cytochrome *b* from 558 nm in membranes of VSMCs (Fig. 2). Since the same spectrum was obtained in non-transfected VSMCs (data not shown), this shift is not caused by plasmid transfection. This peak at ~558 nm exactly reflects the VSMC cytochrome *b* expression, because it was decreased by the disruption of p22^{phox} (Fig. 2). The most likely explanation for the slight shift in the cytochrome peak is that the vascular NADH/NADPH oxidase contains an isoenzyme of cytochrome *b*₅₅₈.

We have previously suggested a functional link between

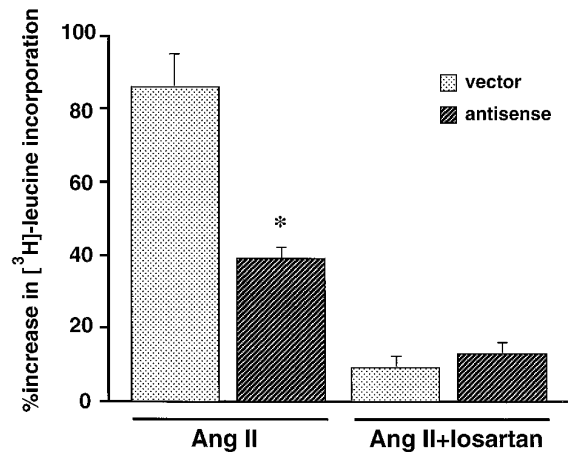


FIG. 4. Angiotensin II-induced hypertrophy in vector- and antisense p22^{phox}-transfected cells and its inhibition by losartan. Bars indicate the percent increase in [³H]leucine incorporation induced by Ang II over the appropriate control. There was no difference in basal incorporation of [³H]leucine between the two cell types. Each bar represents the mean of four independent experiments performed in triplicate. Statistical analysis was performed by one-way analysis of variance. *, *p* < 0.05 for increase by Ang II in antisense- versus vector-transfected cells.

NADH/NADPH oxidase activation and vascular hypertrophy based on the sensitivity of both responses to DPI, an inhibitor of NAD(P)H oxidase (5). However, we could not exclude the nonspecific effects of DPI on other flavoproteins by direct binding (32). In the present study, in p22^{phox}-deficient cells where Ang II-stimulated NADH/NADPH oxidase activity was decreased, Ang II-induced hypertrophy was also decreased (Fig. 4), providing additional support for a central role of this oxidase system in vascular hypertrophy. Interestingly, we also found that the decrease in O₂⁻ production induced by p22^{phox} disruption was accompanied by a decrease in [H₂O₂]_i (Fig. 3B), indicating that Ang II-stimulated H₂O₂ production is mainly through the p22^{phox}-containing NADH/NADPH oxidase activation. Although both O₂⁻ and H₂O₂ have been reported to stimulate VSMC cell growth (7), a recent report indicates that the mitogenic signaling pathways stimulated by these agents are different (33). The present results suggest that at least part of the effect of O₂⁻ on hypertrophy may be mediated by its conversion to H₂O₂.

The functional link between p22^{phox} (cytochrome) expression and NADH/NADPH oxidase activity also seems to be observed *in vivo*, because both p22^{phox} mRNA levels and NADH/NADPH oxidase activities are up-regulated in aortic smooth muscle obtained from rats made hypertensive by Ang II infusion.² Since the luminal narrowing that accompanies hypertension results in part from hypertrophy, the pathways leading to activation of the NADH/NADPH oxidase system, and the factors controlling its expression, may be of potential major significance in the pathogenesis of hypertension.

Thus, the p22^{phox}-deficient VSMCs may be useful for detailed analysis of the p22^{phox}-containing NADH/NADPH oxidase system activated by various agonists and for providing insights into the cellular signaling events involved in vascular cell growth. The identity of the other components and the factors regulating vascular NADH/NADPH oxidase system require further investigation.

² T. Fukui, S. Rajagopalan, N. Ishizaka, J. B. Laursen, Q. Capers IV, W. R. Taylor, D. G. Harrison, H. D. Leon, J. N. Wilcox, and K. K. Griendling, unpublished observations.

Acknowledgments—We thank Dr. Bernard Lassègue for assistance with the phospholipase D assays, Drs. R. Wayne Alexander and David G. Harrison for helpful discussions, and Barbara Merchant-Bailey for editorial assistance.

REFERENCES

- Curnutte, J. T., and Babior, B. M. (1987) *Adv. Hum. Genet.* **16**, 229–297
- Meier, B., Radeke, H. H., Selle, S., Younes, M., Sies, H., Resch, K., and Habermehl, G. G. (1989) *Biochem. J.* **263**, 539–545
- Radeke, H. H., Cross, A. R., Hancock, J. T., Jones, O. T. G., Nakamura, M., Kaefer, V., and Resch, K. (1991) *J. Biol. Chem.* **266**, 21025–21029
- Matsubara, T., and Ziff, M. (1986) *J. Immunol.* **137**, 3295–3298
- Griendling, K. K., Minieri, C. A., Ollerenshaw, J. D., and Alexander, R. W. (1994) *Circ. Res.* **74**, 1141–1148
- Cerutti, P. (1985) *Science* **227**, 375–381
- Rao, G. N., and Berk, B. C. (1992) *Circ. Res.* **70**, 593–599
- Rao, G. N., Lassègue, B., Griendling, K. K., Alexander, R. W., and Berk, B. C. (1993) *Nucleic Acids Res.* **21**, 1259–1263
- Rao, G. N., Lassègue, B., Griendling, K. K., and Alexander, R. W. (1993) *Oncogene* **8**, 2759–2764
- Tsai, J.-C., Jain, M., Hsieh, C.-M., Lee, W.-S., Yoshizumi, M., Patterson, C., Perrella, M. A., Cooke, C., Wang, H., Haber, E., Schlegel, R., and Lee, M.-E. (1996) *J. Biol. Chem.* **271**, 3667–3670
- Nunoi, H., Rotrosen, D., Gallin, J. I., and Malech, H. L. (1988) *Science* **242**, 1298–1301
- Volpp, B. D., Nauseef, W. M., and Clark, R. A. (1988) *Science* **242**, 1295–1297
- Abo, A., Pick, E., Hall, A., Totty, N., Teahan, C. G., and Segal, A. W. (1991) *Nature* **353**, 668–670
- Knaus, U. G., Heyworth, P. G., Kinsella, B. T., Curnutte, J. T., and Bokoch, G. M. (1992) *J. Biol. Chem.* **267**, 23575–23582
- Parkos, C. A., Allen, R. A., Cochrane, C. G., and Jesaitis, A. J. (1987) *J. Clin. Invest.* **80**, 732–742
- Meier, B., Cross, A. R., Hancock, J. T., Kaup, F. J., and Jones, O. T. G. (1991) *Biochem. J.* **275**, 241–245
- Jones, O. T. G., Jones, S. A., Hancock, J. T., and Topley, N. (1993) *Biochem. Soc. Trans.* **21**, 343–346
- Meier, B., Jesaitis, A. J., Emmendorffer, A., Roesler, J., and Quinn, M. T. (1993) *Biochem. J.* **289**, 481–486
- Neale, T. J., Ullrich, R., Ojha, P., Poczewski, H., Verhoeven, A. J., and Kerjaschki, D. (1993) *Proc. Natl. Acad. Sci. U. S. A.* **90**, 3645–3649
- Jones, O. T. G. (1994) *Bioessays* **16**, 919–923
- Steinbeck, M. J., Appel, W. H., Jr., Verhoeven, A. J., and Karnovsky, M. J. (1994) *J. Cell Biol.* **126**, 765–772
- Jones, S. A., Hancock, J. T., Jones, O. T. G., Neubauer, A., and Topley, N. (1995) *J. Am. Soc. Nephrol.* **5**, 1483–1491
- Mohazzab-H, K. M., Kaminski, P. M., and Wolin, M. S. (1994) *Am. J. Physiol.* **266**, H2568–H2572
- Mohazzab-H, K. M., and Wolin, M. S. (1994) *Am. J. Physiol.* **267**, L823–L831
- Fukui, T., Lassègue, B., Kai, H., Alexander, R. W., and Griendling, K. K. (1995) *Biochim. Biophys. Acta* **1231**, 215–219
- Griendling, K. K., Taubman, M. B., Akers, M., Mendlowitz, M., and Alexander, R. W. (1991) *J. Biol. Chem.* **266**, 15498–15504
- Lassègue, B., Alexander, R. W., Nickenig, G., Clark, G., Murphy, T. J., and Griendling, K. K. (1995) *Mol. Pharmacol.* **48**, 601–609
- Ohba, M., Shibamura, M., Kuroki, T., and Nose, K. (1994) *J. Cell Biol.* **126**, 1079–1088
- Dinauer, M. C., Pierce, E. A., Bruns, G. A., Curnutte, J. T., and Orkin, S. H. (1990) *J. Clin. Invest.* **86**, 1729–1737
- Leto, T. L., Adams, A. G., and de Mendez, I. (1994) *Proc. Natl. Acad. Sci. U. S. A.* **91**, 10650–10654
- Maly, F. E., Schuerer-Mayl, C. C., Quilliam, L., Cochrane, C. G., Newburger, P. E., Curnutte, J. T., Gifford, M., and Dinauer, M. C. (1993) *J. Exp. Med.* **178**, 2047–2053
- Majander, A., Finel, M., and Wikstrom, M. (1994) *J. Biol. Chem.* **269**, 21037–21042
- Baas, A. S., and Berk, B. C. (1995) *Circ. Res.* **77**, 29–36